

## EVALUATION OF VEHICLE ENGINE THERMAL ENERGY SYSTEM DETECTION EFFECT BASED ON TARGET DETECTION ALGORITHM

by

**Jie HAN<sup>a</sup>, Yang LIU<sup>a\*</sup>, Hao FENG<sup>a</sup>, and Sha YANG<sup>b</sup>**

<sup>a</sup> Faculty of Information Science and Engineering, Wuhan College, Wuhan, China

<sup>b</sup> Department of Computer Science and Technology, Hankou University, Wuhan, China

Original scientific paper

<https://doi.org/10.2298/TSCI2104031H>

*The paper takes the front-mounted parallel structure of the transmission as an example and uses the target detection algorithm to introduce a real-time equivalent energy consumption control strategy for the vehicle engine thermal energy system. Based on studying the relationship between fuel thermal energy and electrical energy consumed when the vehicle is driving in a cycle, we elaborated on the strategy's critical issue, namely, the equivalent method of the electrical energy of the battery pack and the fuel thermal energy consumption of the engine. Finally, the thesis carries out a simulation test on this strategy based on the vehicle simulation model and compares it with other control strategies.*

**Key words:** *target detection algorithm, thermal energy system detection, equivalent energy consumption, control strategy, vehicle engine, modelling and simulation*

### Introduction

At present, the optimization methods of hybrid electric vehicle (HEV) control strategies are mainly divided into global optimization and real-time optimization. Global optimization is generally multi-level decision-making of energy flow control for a specific working condition cycle. The application range of the optimization results has significant limitations. It is difficult to apply to the actual control [1]. Real-time optimization is only optimized for the energy flow control of the vehicle's instantaneous operating conditions and is not subject to the overall restriction of the specific operating cycle. Therefore, the optimization results can be easily applied to the actual control of HEV.

Taking a parallel charge-maintaining HEV as an example, a target detection algorithm introduces a vehicle engine thermal energy real-time equivalent energy consumption minimum control strategy (ECMS). This strategy optimizes the power distribution of the engine and the motor under various transient operating conditions. The vehicle's total energy consumption per unit time (including the actual fuel heat energy consumption and the electric energy consumption of the battery pack) is minimized, and the battery state of charge (SOC) is maintained. Since the battery power of the charge-maintained HEV comes from the fuel heat, the fuel thermal energy consumption of the engine and the electrical energy consumption of the battery pack (positive and negative) must be attributed to a unified energy consumption index in a certain way, that is, the vehicle engine thermal energy, *etc.* Effective energy consumption index [2]. The author adopts a method of introducing *equivalent factor* to equalize electric energy

\* Corresponding author, e-mail: lyforever\_15@163.com

consumption and fuel thermal energy consumption and establishes an objective function aiming to minimize the *real-time equivalent energy consumption of vehicle engine thermal energy*, combined with the vehicle simulation model the related constraints included are solved. Finally, the optimization results are verified by simulation.

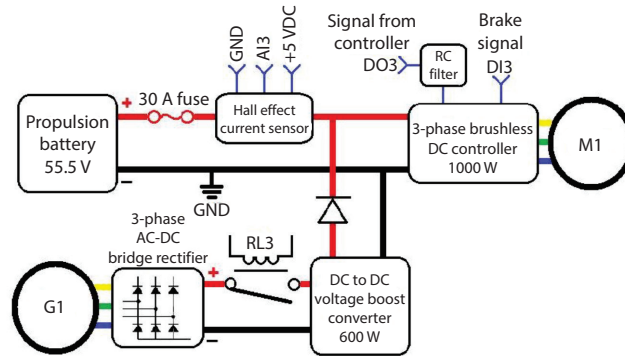


Figure 1. Transmission front-mounted parallel structure

### Real-time equivalent energy minimum strategy

#### The HEV structure and mathematical system model

Figure 1 shows the front-mounted parallel structure of the transmission. In this structure, the energy flow is divided into two paths: the engine one, the fuel heat is converted into mechanical energy flow; the motor one, the electrical energy is converted into mechanical energy flow, and the two mechanical energy is collected at the combiner box [3]. The vehicle parameters are shown in tab. 1, where the motor can be overloaded by 2.5 times in a short time, and the automatic transmission ratios are 6.195, 3.895, 2.26, 1.428, and 1.

Table 1. Vehicle parameters

Total weight [kg]	1400	Battery pack capacity [Ah]	100×29
Engine power [kW]	87	Main transmission ratio	6.833
Motor power [kW]	55	Motor reduction ratio	1.667
Air resistance coefficient	0.5	Wheel radius [m]	0.493
Rolling resistance coefficient	0.015	Windward area [m <sup>2</sup> ]	7.25

At time  $t$ , the kinematics and dynamics of the motor, engine, and wheels:

$$\omega_w(t) = \frac{\omega_e(t)}{R_e(t)} = \frac{\omega_m(t)}{R_m} \quad (1)$$

$$T_w(t) = R_e(t)T_e(t) + R_m T_m(t) \quad (2)$$

where  $\omega_w$  is the wheel speed,  $\omega_e$  – the engine speed,  $\omega_m$  – the motor speed,  $T_w$  – the wheel torque,  $T_e$  – the engine torque,  $T_m$  – the motor torque,  $R_e$  – the transmission ratio, and  $R_m$  – the motor reduction ratio.

#### Optimize standard functions

In eqs. (1) and (2), the wheel speed and torque demand  $\omega_w[t], T_w(t)$  are known, and the output torque of the engine and the motor are variable. Define the ratio of  $T_w$  to the engine

one way as  $u$ , then the output torque of  $u(t) = T_e(t)R_e(t)/T_w(t)$  engine and motor are  $u(t)T_w(t)R_e(t)$  and  $[1 - u(t)]T_w(t)R_m$ , respectively.

### Objective function

The real-time equivalent energy consumption minimization strategy of vehicle engine thermal energy is to minimize the total energy consumed by the vehicle per unit time by optimizing the value of  $u$  under each instantaneous operating condition. Since the conversion efficiency between electrical energy and mechanical energy is much higher than that between thermal fuel energy and mechanical energy, if the direct addition of electrical energy and fuel thermal energy as the total energy consumption index is optimized, it will consume electrical energy [4]. The way to solve this problem is to introduce an *equivalent factor*  $S(t)$  to *equivalent* the electrical energy consumed (supplemented) by the battery and the thermal fuel energy. At this time, the objective function of the vehicle's instantaneous energy consumption can be expressed:

$$\min J[u(t), R_e(t)] = \Delta E_e[u(t), \omega_e(t)] + S(t)\Delta E_b[u(t), \omega_m(t)] \quad (3)$$

where  $\Delta E_e[u(t), \omega_e(t)]$ ,  $\Delta E_b[u(t), \omega_m(t)]$  is the energy consumed by the engine and motor in the optimized time step  $\Delta t$ :

$$\Delta E_e[u(t), \omega_e(t)] = H_u mf [u(t), \omega_e(t)] \Delta t \quad (4)$$

$$\Delta E_b[u(t), \omega_m(t)] = I_b [u(t), \omega_m(t)] V_b [u(t), \omega_m(t)] \Delta t \quad (5)$$

where  $H_u$  is the low heating value of the fuel,  $mf$  – the fuel consumption rate,  $I_b$ ,  $V_b$ , and  $C$  are the current and open-circuit voltage of the battery, which are related to the torque and speed of the motor.

### Mechanical constraints

Restricted by mechanical constraints, the output torque  $T_e$ ,  $T_m$  and speed  $\omega_e$ ,  $\omega_m$  of the engine and motor in the structure of fig. 1 can only vary within a specific range. The speed constraint:

$$\omega_{e\_min} \leq \omega_e(t) \leq \omega_{e\_max}, \quad 0 \leq \omega_m(t) \leq \omega_{m\_max} \quad (6)$$

The torque constraints:

$$\begin{aligned} 0 \leq T_e(t) \leq T_{e\_max}[\omega_e(t)] \\ T_{m\_min}[\omega_m(t)] \leq T_m(t) \leq T_{m\_max}[\omega_m(t)] \end{aligned} \quad (7)$$

Since the wheel speed and torque demand at time,  $t$ , are known, the mechanical constraints can be simplified by combining eqs. (1) and (2).

### Simplified speed constraints

From eq. (1), it can be seen that under the premise of a constant  $\omega_w$ , the output speed  $\omega_m$  of the motor is a fixed value, and the output speed  $\omega_e(t)$  of the engine is determined by the transmission speed ratio  $R_e(t)$  so that the speed constraint condition can be simplified to the set  $R_e(t) \in R(t)$  of the speed ratio.

Where  $R_e$  is a set of selectable transmission gears that meet the following conditions:

- the speed requirements of the engine and the motor should be within the actual speed range that can be achieved and
- the  $T_w(t)$  should be less than or equal to the maximum torque that the transmission system can deliver range.

**Simplified torque constraint conditions**

Substituting engine and motor output torques  $u(t)T_w(t)/R_e(t)$  and  $[1 - u(t)]T_w(t)/R_m$  into eq. (7), the torque constraint condition is simplified to the constraint condition of  $u(t)$ :

$$u(t) > \max \left[ \frac{T_{e\_min} R_e(t)}{T_w}, \frac{T_w - T_{m\_max} R_m}{T_w} \right]$$

$$u(t) > \min \left[ \frac{T_{e\_max} R_e(t)}{T_w}, \frac{T_w - T_{m\_min} R_m}{T_w} \right]$$
(8)

In summary, the standard equation of the optimization function can be expressed:

$$\min J[u(t), R_e(t)] = \Delta E_e[u(t), R_e(t)] + S(t)\Delta E_b[u(t)]$$

$$Stu(t) > \max \left[ \frac{T_{e\_min} R_e(t)}{T_w}, \frac{T_w - T_{m\_max} R_m}{T_w} \right]$$

$$u(t) > \min \left[ \frac{T_{e\_max} R_e(t)}{T_w}, \frac{T_w - T_{m\_min} R_m}{T_w} \right]$$

$$R_e(t) \in R(t)$$
(9)

The realization process of the real-time equivalent energy minimum strategy is shown in fig. 2. In the step  $\Delta(t)$  at time  $t$ , the optimal value  $u_{opt}(t)$ ,  $R_{eopt}(t)$  of the variable  $u(t)$ ,  $R_e(t)$  is found by optimizing the  $J[u(t), R_e(t)]$  function.

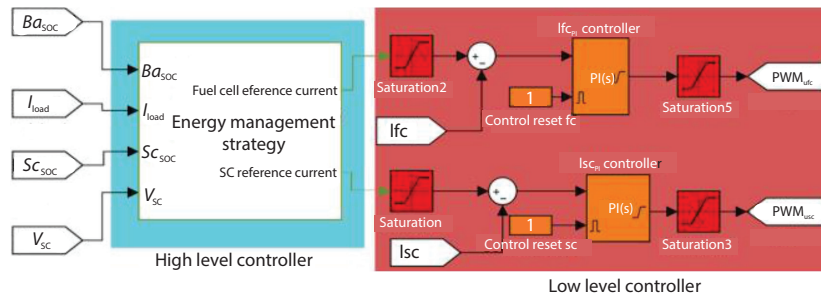


**Figure 2. The ECMS workflow**

**Target detection algorithm**

The target detection algorithm’s principle is to use random update and neighborhood update mechanisms in background modelling, which mainly includes three modules: background template initialization, target detection, and background template update [5].

$V^1(x)$	$V^2(x)$	$V^3(x)$
$V^4(x)$	$V(x)$	$V^5(x)$
$V^6(x)$	$V^7(x)$	$V^8(x)$

**Figure 3. Eight-neighborhood model**

**Background template initialization**

Each pixel of the first frame of the sequence image selects a pixel from its eight-neighborhood model (shown in fig. 3) and saves it into its background template, repeating  $N$  times. Note that the European color space value at the pixel  $x$  is  $V(x)$ , and the template  $M(x) = \{V_1, V_2, V_3, \dots, V_N\}$  established by the background is the pixel value in the background sample space.

**Target detection**

The target detection algorithm divides the new pixel  $V(x)$  at this position according to the background model  $M(x)$  corresponding to each pixel. As shown in fig. 4,  $C_1, C_2$  is the color moment, which defines a sphere  $S_R[V(x)]$  with the pixel  $V(x)$  as the center and  $R$  as the radius. Calculate the Euclidean distance of  $N$  samples in  $V(x)$  and  $M(x)$ , and judge whether the current pixel belongs to the moving target or the background according to the number of intersections of  $M(x)$  and  $S_R[V(x)]$ .

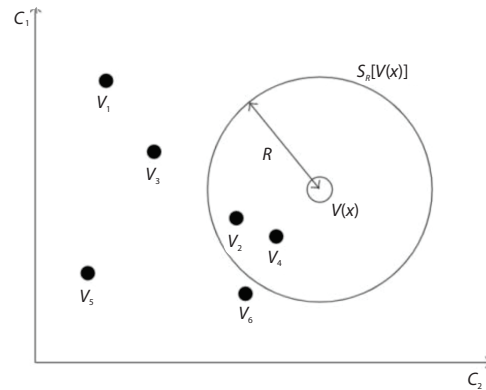


**Figure 4. The ViBe classification model**

**Background template update**

In the template update, this article adopts a conservative update strategy. When the pixel  $V(x)$  is judged to be a background, a value in the background sample  $M(x)$  is randomly selected during the update process and replaced with  $V(x)$ , and the background template sample value of the  $V(x)$  neighborhood is also updated with equal probability [6]. Assuming that time is continuous, after  $dt$  time, the probability that the template sample changes with time is shown:

$$P(t, t + dt) = e^{-\ln(N/N-1)dt} \tag{10}$$

It can be seen that the sample update has nothing to do with time, and the sampling method is memoryless, which improves the dynamic adaptability of the algorithm [7].

**Selection of equivalent factor**

Equivalent factor  $S(t)$  is the weight of electric energy consumption in formula (3), and how to determine its magnitude is the key to ECMS. If  $S(t)$  is too large, it means that the consumption of electric energy will be excessively punished, and the work opportunities of fuel will increase, which will lead to an increase in fuel consumption. Similarly, if  $S(t)$  is too small, it will lead to battery power. Excessive consumption.

**The equivalent relationship between fuel thermal energy and electrical energy in cycle conditions**

Carrying out multiple simulation tests on an individual working condition cycle with different  $u$  values, the energy consumption  $[E_e(u), E_b(u)]$  of fuel oil heat energy and battery electric energy corresponding to different  $u$  values under this working condition cycle can be obtained. Here, the parallel HEV shown in fig. 1 is driven under the ETC urban cycle condition as an example for the simulation test [8]. The  $u$  value range is set to 0.7~1.5, and the step length  $\Delta u$  is 0.05. Figure 5 shows each  $u$  after the simulation. The relationship between the fuel thermal energy  $E_e$  and electric energy  $E_b$  corresponding to the value. It can be seen from fig. 5 that  $u = 1$  (that is, pure engine working mode) divides the curve into two linear segments. When  $u > 1$  the thermal fuel energy is surplus, the battery is working in a charged state, at this  $E_b/E_{b1}, u < 1$ , when the thermal fuel energy is insufficient, the battery needs to provide extra energy, At this time  $E_b > E_{b1}$ . Therefore, the relationship between fuel thermal energy consumption and battery power consumption can be expressed:

$$E_e = f(E_b) = \begin{cases} E_{e1} - S_{\text{chg}}(E_b - E_{b1})E_b < E_{b1} \\ E_{e1} - S_{\text{dis}}(E_b - E_{b1})E_b < E_{b1} \end{cases} \quad (11)$$

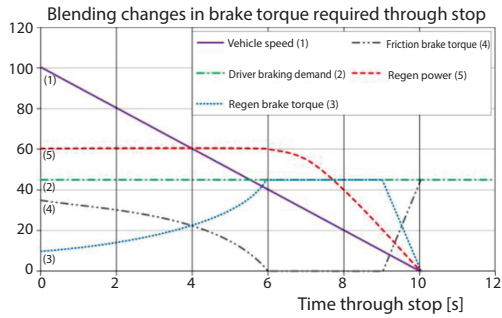


Figure 5. The  $E_e = f(E_b)$  relationship obtained in ETC

where  $E_{e1}$ ,  $E_{b1}$  are the fuel heat energy consumed and the electric energy recovered by braking into the battery when  $u = 1$  (pure engine drive mode), and  $S_{\text{chg}}$ ,  $S_{\text{dis}}$  are the absolute values of the slopes of the two straight lines in fig. 5, respectively.

From the equivalence perspective, the change in electric energy must be compensated by the corresponding change in fuel thermal energy. That is, consuming/replenishing a certain amount of electric energy can be equivalent to consuming/saving a certain amount of thermal fuel energy [9]. Suppose the amount of

electrical energy change is,  $E_b$ , and the compensation amount of thermal fuel energy is  $\zeta(E_b)$ . Next, the equivalent functional relationship between  $E_b$  and  $\zeta(E_b)$  is explained in conjunction with figs. 6(a) and 6(b). If the electrical energy change is  $E_b$  (indicated by the white arrow in fig. 6), then the electrical energy that needs to be compensated by thermal fuel energy is  $-(E_b - E_{b1})$  (the black arrow in fig. 6). As shown in eq. (10), it can be seen that when the electric energy consumption is  $-(E_b - E_{b1})$ , the corresponding fuel thermal energy consumption is  $f(E_{b1} - E_b)$ . Since the fuel thermal energy consumption corresponding to the electrical energy change  $E_{b1}$  is  $E_{e1}$ , the fuel thermal energy compensation required for the electrical energy change  $E_b$  at this time, The quantity  $\zeta(E_b)$  can be expressed as the difference between  $f(E_{b1} - E_b)$  and the fuel thermal energy consumption  $E_{e1}$  in pure engine mode:

$$\zeta(E_b) = f(E_{b1} - E_b) - E_{e1} \quad (12)$$

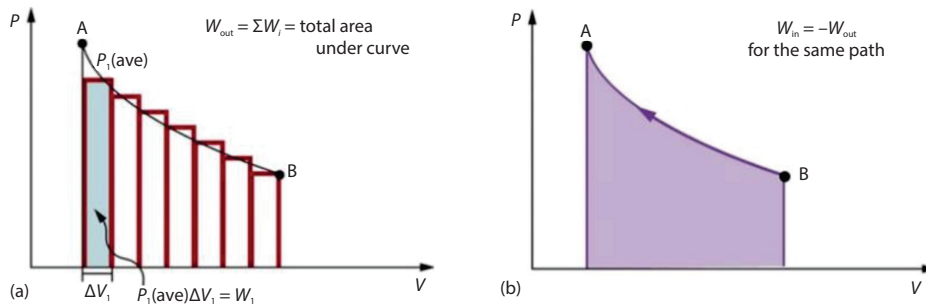


Figure 6. The relationship between electrical energy  $E_b$  and equivalent fuel oil thermal energy  $\zeta(E_b)$

The paper substitutes eq. (12) into eq. (11) to obtain the equivalent relationship between fuel heat energy and battery electric energy:

$$\zeta(E_b) = \begin{cases} S_{\text{chg}} E_b & E_b > 0 \\ S_{\text{dis}} E_b & E_b < 0 \end{cases} \quad (13)$$

The aforementioned conclusions can also be obtained from the simulation test of UK-BUS, WVUCITY, ECE, and other paper cycle conditions. The value of  $S_{\text{chg}}$ ,  $S_{\text{dis}}$  and the aver-

**Table 2. Corresponding  $S_{\text{chg}}$ ,  $S_{\text{dis}}$  values under different working conditions**

Working condition	$P_{\text{an}}$ [kW]	$S_{\text{chg}}$	$S_{\text{dis}}$
UKBUS	9.0722	5.2489	1.7179
WVUCITY	9.5046	5.0074	1.7097
ECE	12.7994	4.7307	1.7391
ETC (city segment)	14.9849	3.8442	1.7311

age power demand,  $P_{\text{mean}}$ , of the operating conditions obtained by the simulation are shown in tab. 2. From the table, it can be found that the different cycle conditions  $S_{\text{chg}}$ ,  $S_{\text{dis}}$  obtained below is not the same, and its value should be related to the characteristics of the working condition.

**Selection of real-time equivalent factor**

The aforementioned research can be found  $S_{\text{chg}}$  and  $S_{\text{dis}}$  have the same meaning as the equivalent factor. If the driving time of a particular working condition is the time step  $\Delta t$  of real-time optimization, then eq. (13) can be applied to real-time optimization [10]. Now starting from the two working states of battery pack charging and discharging,  $S_{\text{chg}}$  and  $S_{\text{dis}}$  are selected.

*The value of  $S_{\text{chg}}$*

Fuel thermal energy and electric energy (oil-to-electricity for short) conversion use the engine-generator set as an energy converter to convert the thermal fuel energy into electrical energy and store it in the battery pack. It can be seen from fig. 3 that the ratio of the stored unit electric energy to the fuel heat energy consumed is the reciprocal of  $S_{\text{chg}}$ , then  $S_{\text{chg}}$  at time  $t$ :

$$S_{\text{chg}}(t) = \frac{1}{[\eta_e(t)\eta_T(t)\eta_c(t)]} \tag{14}$$

where  $\eta_e$  is the practical efficiency of the engine generator set,  $\eta_c$  – the charging efficiency of the battery, and  $\eta_T$  – the mechanical transmission efficiency of the oil-to-electric conversion branch.

*The value of  $S_{\text{dis}}$*

Although the energy flow path of converting fuel into electric energy is irreversible, the consumption of fuel will be correspondingly reduced when the electric energy is consumed [11]. From fig. 3, it can be seen that the ratio of the consumed unit electric energy to the saving fuel heat energy is the reciprocal of  $S_{\text{dis}}$ , then  $S_{\text{dis}}$  at time  $t$ :

$$S_{\text{dis}}(t) = \frac{\eta_e(t)\eta_T(t)}{\eta_d(t)} \tag{15}$$

where  $\eta_d$  is the discharge efficiency of the battery. In the drive system, each component’s work efficiency changes non-linearly with the change of the operating point. Considering the average effect produced by a large number of different operating points in the driving conditions of the car, the eqs. (14) and (15), Can use average efficiency.

**Correction of equivalence factor**

The operating range of the battery pack *SOC* in the battery-maintaining HEV is usually set to 0.5-0.9, and it is expected to work around an average value of 0.7 (predetermined value). If the *SOC* deviates from the predetermined value, the battery pack’s operating point needs to be changed by appropriate adjustment and correction of the identical factor. The specific method: use eq. (16) to standardize the *SOC* to  $SOC_b$  ( $-1 \sim 1$ ), and then use the correction function correct the identical factor:

$$\Delta SOC_b = \begin{cases} 1 & SOC \geq SOC_h \\ SOC - \frac{SOC_h + SOC_l}{2} & SOC_h > SOC > SOC_l \\ -1 & SOC \leq SOC_l \end{cases} \quad (16)$$

where  $SOC_h$ ,  $SOC_l$  and, respectively, are the upper and lower limits of the operating range of the battery pack  $SOC$ . The correction function should have the following characteristics:

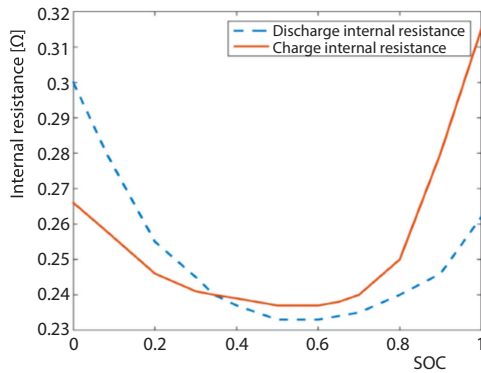


Figure 7. The S-shaped equivalent factor correction curve for SOC

- when  $\Delta SOC_b$  is more significant than, equal to, or less than zero, the function outputs values more significant than, equal to, or less than 1, respectively,
- when  $\Delta SOC_b$  is near zero, the function value changes smoothly, and
- when  $\Delta SOC_b$  deviates from zero.

When far, the function value quickly reaches the set maximum (small) value. Sigmoid function  $E K(SOC) = 1 - a \Delta SOC_b^3 + b \Delta SOC_b^4$ . It is a function that satisfies the aforementioned characteristics [12]. This function is composed of a third-order curve and a fourth order curve function. The shape of the curve can be changed by changing the weights  $[a, b]$ . Figure 7 shows the use of different  $[a, b]$  S-shaped curve at the value.

**Improved real-time equivalent energy minimum strategy**

Based on the previous content, the objective function of the final real-time equivalent energy minimum strategy can be changed:

$$\begin{aligned} \min J[u(t), R_e(t)] &= \begin{cases} \Delta E_e[u(t), R_e(t)] - K(SOC)\Delta E_b[u(t)] / [\eta_e(t)\eta_r(t)\eta_c(t)], & \Delta E_b > 0 \\ \Delta E_e[u(t), R_e(t)] - K(SOC)\Delta E_b[u(t)]\eta_d(t) / [\eta_e(t)\eta_r(t)], & \Delta E_b < 0 \end{cases} \\ S.t. u(t) &> \max \left[ \frac{T_{e\_min} R_e(t)}{T_w}, \frac{T_w - T_{m\_max} R_m}{T_w} \right] \\ u(t) &> \min \left[ \frac{T_{e\_max} R_e(t)}{T_w}, \frac{T_w - T_{m\_min} R_m}{T_w} \right] \\ R_e(t) &\in R(t) \end{aligned} \quad (17)$$

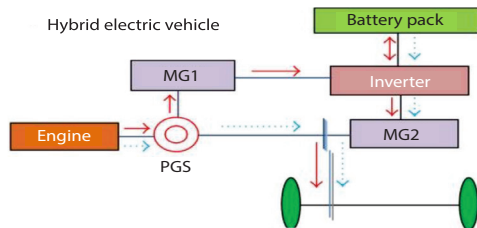


Figure 8. The optimization process of using ECMS in HEV

Figure 8 shows the application process of ECMS in HEV, where  $\alpha(t)$ ,  $\beta(t)$ ,  $\gamma(t)$  is the operating state of the accelerator pedal, brake, and clutch, respectively, and  $u_{opt}(t)$ ,  $R_{eopt}(t)$  is the optimal output torque of the engine and motor, respectively [13].

### Simulation of the control strategy

Based on the MATLAB/SIMULINK platform [14], taking the structure of fig. 1 as an example, a simulation model is established according to the process of fig. 8 based on the mathematical model, and the vehicle speed  $v(t)$  and acceleration  $a(t)$  are input for real-time simulation. The simulation step size  $\Delta t$  is set = 1 second. The optimal distribution ratio  $u_{opt}(t)$  and the optimal transmission ratio  $R_{eopt}(t)$  obtained by real-time optimization when the initial SOC is 0.7 are shown in fig. 9. The SOC change curves were obtained with different initial SOC values (0.6, 0.7, and 0.8), as shown in fig. 10. Taking UKBUS, WVUCITY, ECE, ETC, and other cycles as vehicle driving target conditions, simulation tests were carried out, respectively. The fuel economy comparison between this control strategy and the motor-assisted control strategy in ADVISOR and the HEV fuel economy using a 183 kW engine alone to drive similar conventional cars are shown in tab. 3.

It can be seen from tab. 3 that the parallel HEV adopts the real-time minimum energy consumption control strategy in the article to improve the fuel economy of the motor-assisted control strategy by about 26%, 17%, *etc.*, respectively in UKBUS, WVUCITY, ECE, ETC, and other operating conditions. Compared with pure engine, 12%, 11%, and 14% are increased by about 35%, 29%, 35%, 28%, and 30%, respectively. Figures 9 and 10 illustrate that the control strategy can be applied in real-time driving conditions, and the battery pack SOC falls within the design range of 0.5-0.9.

### Conclusion

Based on the study of the relationship between fuel thermal energy and electrical energy when the vehicle is running in a cycle, the paper finds a better method of equivalent electrical energy and (fuel) thermal energy, which solves the problem of the vehicle engine thermal energy real-time equivalent energy consumption minimum control strategy unification of indicators. From the analysis of the research results, the real-time equivalent energy con-

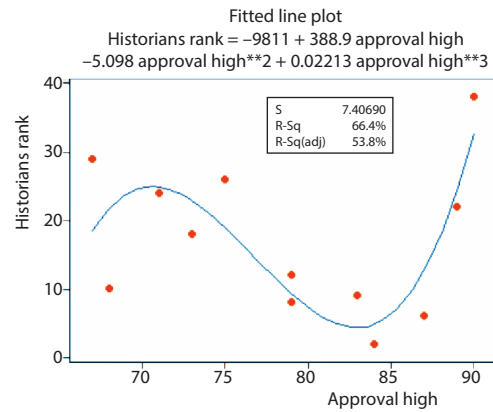


Figure 9. The best control variables  $u_{opt}(t)$ ,  $R_{eopt}(t)$  obtained by real-time optimization

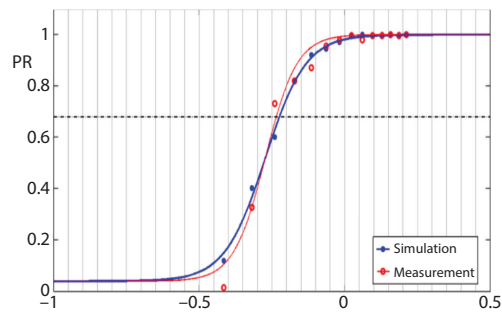


Figure 10. The SOC variation curve obtained by simulation

Table 3. Corresponding engine fuel consumption under different control strategies

Working condition	In the text	Advisor	Pure engine
UKBUS	28.16	37.92	43.38
WVUCITY	29.48	35.30	41.42
ECE	26.41	30.06	40.48
ETC	24.45	27.60	33.94
ETC+WVUCITY	26.97	31.3	38.38

sumption minimum control strategy of vehicle engine thermal energy is an energy management method that can be practically applied in hybrid electric vehicles. The better optimization effect is to reduce vehicle fuel consumption. The thesis's research also found that the driving condition characteristics and the identical factor and the improvement of fuel economy have a certain correlation, which needs to be studied in-depth, such as establishing the equivalent factor and the adaptive model of the operating condition.

### Acknowledgment

The project was supported by Hubei Key Laboratory of Big Data in Science and Technology (Wuhan Library of Chinese Academy of Science) (Grant No.20KF011009) and Hubei Provincial Natural Science Foundation of China (Grant No.ZRMS2019001565).

### References

- [1] Yu, W., et al., An Efficient Top- $k$  Ranking Method for Service Selection Based on  $\varepsilon$ -ADMOPSO Algorithm, *Neural Computing and Applications*, 31 (2019), 1, pp. 77-92
- [2] Ghosh, R., et al., Performance Evaluation of a Real-Time Seismic Detection System Based on CFAR Detectors, *IEEE Sensors Journal*, 20 (2019), 7, pp. 3678-3686
- [3] Ketz, N., et al., Closed-Loop Slow-Wave tACS Improves Sleep-Dependent Long-Term Memory Generalization by Modulating Endogenous Oscillations, *Journal of Neuroscience*, 38 (2018), 33, pp. 7314-7326
- [4] Wu, S., Construction of Visual 3-D Fabric Reinforced Composite Thermal Performance Prediction System, *Thermal Science*, 23 (2019), 5, pp. 2857-2865
- [5] Kao, I. H., et al., Analysis of Permanent Magnet Synchronous Motor Fault Diagnosis Based on Learning, *IEEE Transactions on Instrumentation and Measurement*, 68 (2018), 2, pp. 310-324
- [6] Filippini, F., et al., Experimental Results of Polarimetric Detection Schemes for DVB-T-Based Passive Radar, *IET Radar, Sonar & Navigation*, 11 (2017), 6, pp. 883-891
- [7] Yu, W., Li, S., Recommender Systems Based on Multiple Social Networks Correlation, *Future Generation Computer Systems*, 87 (2018), Oct., pp. 312-327
- [8] Shen, M., Gao, Q., A Review on Battery Management System from the Modelling Efforts to Its Multi-Application and Integration, *International Journal of Energy Research*, 43 (2019), 10, pp. 5042-5075
- [9] Malyuta, D., et al., Long-Duration Fully Autonomous Operation of Rotorcraft Unmanned Aerial Systems for Remote-Sensing Data Acquisition, *Journal of Field Robotics*, 37 (2020), 1, pp. 137-157
- [10] Kiyabu, S., et al., Computational Screening of Hydration Reactions for Thermal Energy Storage: New Materials and Design Rules, *Chemistry of Materials*, 30 (2018), 6, pp. 2006-2017
- [11] Choi, W., et al., Voltageids: Low-Level Communication Characteristics for Automotive Intrusion Detection System, *IEEE Transactions on Information Forensics and Security*, 13 (2018), 8, pp. 2114-2129
- [12] McTaggart-Cowan, G., et al., Impacts and Mitigation of Varying Fuel Composition in a Natural Gas Heavy-Duty Engine, *SAE International Journal of Engines*, 10 (2017), 4, pp. 1506-1517
- [13] Luise, F., et al., Design Optimization and Testing of High-Performance Motors: Evaluating a Compromise between Quality Design Development and Production Costs of a Halbach-Array PM Slotless Motor, *IEEE Industry Applications Magazine*, 22 (2016), 6, pp. 19-32
- [14] Wu, S., Study and Evaluation of Clustering Algorithm for Solubility and Thermodynamic Data of Glycerol Derivatives, *Thermal Science*, 23 (2019), 5, pp. 2867-2875